Gene Expression, Biodistribution, and Pharmacoscintigraphic Evaluation of Chondroitin Sulfate—PEI Nanoconstructs Mediated Tumor Gene Therapy

Atul Pathak,[†] Pradeep Kumar,[†] Krishna Chuttani,[‡] Sanyog Jain,[‡] Anil K. Mishra,[‡] Suresh P. Vyas,[§] and Kailash C. Gupta[†,∥,*]

[†]Institute of Genomics and Integrative Biology (CSIR), Delhi University Campus, Mall Road, Delhi-110007, India, [‡]Institute of Nuclear Medicine and Allied Science, Delhi-110009, India, [§]Department of Pharmaceutical Sciences, Dr. Harisingh Gour Vishwavidyalaya, Sagar-470003, M.P., India, and [∥]Indian Institute of Toxicology Research, M.G. Road, Post Box No. 80, Lucknow-226001, U.P., India

ABSTRACT Tumor-specific gene delivery constitutes a primary challenge in nonviral mediated gene therapy. In this investigation, branched polyethylenimine (bPEI, 25 kDa) was modified by forming nanoconstructs with a natural polysaccharide, chondroitin sulfate (CS), to impart site-specific property. A library of CS—PEI (CP) nanoconstructs was fabricated by altering the content of CS and evaluated in terms of size, surface charge, morphology, pDNA loading efficiency, pDNA release assay, pDNA protection study, cytotoxicity, and transfection efficiency. *In vitro* transfection efficiency of CP nanoconstructs was examined in HEK293, HEK293T, HepG2, and HeLa cell lines, while their cytotoxicity was investigated in HepG2 and HeLa cells. DNase I protection assay showed that the plasmid was protected from degradation over a period of time. The CP nanoconstructs possess significantly lower toxicity and enhanced transfection efficiency compared to PEI (25 kDa) and commercial transfection reagents (*i.e.*, superfect, fugene, and GenePORTER 2). Further, the CP nanoconstructs were also found to transfect cells in serum-containing medium. *In vivo* studies were carried out with pDNA loaded CP-3 nanoconstruct after intravenous (iv) injection in Ehrlich ascites tumor (EAT)-bearing mice. The outcome revealed higher concentration of CP-3 nanoconstruct in tumor mass. These findings demonstrate that CP nanoconstructs could be exploited as carriers for nanomedicine for efficient management of solid tumor.

KEYWORDS: PEI · chondroitin sulfate · transfection · cytotoxicity · biodistribution · solid tumor

Recently, gene therapy has witnessed much enthusiasm among researchers for correcting human genetic disorders.[1] The ability of the therapeutics to mediate target-specific delivery to tumor cells remains one of the most important unmet goals in gene therapy. This aspect still remains an area of concern along with clinical applications of DNA-based therapeutics to treat tumors in want of safe and competent delivery systems. The nonviral gene carriers (*e.g.*, liposomes, nanoparticles, dendrimers, *etc.*) are drawing substantial attention due to their stability, ease of preparation, and safety and could represent an attractive approach to developing gene therapy for treatment of numerous acquired or inherited human diseases.[2−6] Other alternative delivery methods like viral carriers have some serious drawbacks, though; viral carriers (*e.g.*, retrovirus, adenovirus, *etc.*) are far superior to nonviral gene delivery systems in terms of transfection efficiency.[7,8] However, due to safety concerns, pharmaceutical applications of a viral vector are not in much evident. Ideally, a gene carrier should condense DNA into the particles, crossing the permeability barrier of the cell, and finally relocate the DNA into the nucleus for protein expression. Among nonviral vectors, polyethylenimine (PEI), *viz.*, branched (25 kDa) and linear (25 kDa), is a commercially available polymeric gene transfer agent which has been successfully used for gene delivery both *in vitro* and *in vivo*.[9,10] The PEI contains primary, secondary, and tertiary amines in a ratio of 1:2:1 that become protonated in an acidic environment of endosome giving rise to "proton sponge effect".[11] This may protect the DNA from degradation in the endosomal compartment during the maturation of the endosome to lysosome, facilitating intracellular trafficking of DNA. High charge density of PEI also contributes to the formation of highly condensed particles by interacting with DNA. This property may have been associated with problems in *in vivo* conditions, cytotoxicity, nonspecific interactions with nontarget tissues, and blood components. In order to overcome these

*Address correspondence to kcgupta@igib.res.in.

Received for review January 16, 2009 and accepted May 07, 2009.

Published online May 18, 2009.
10.1021/nn900044f CCC: $40.75

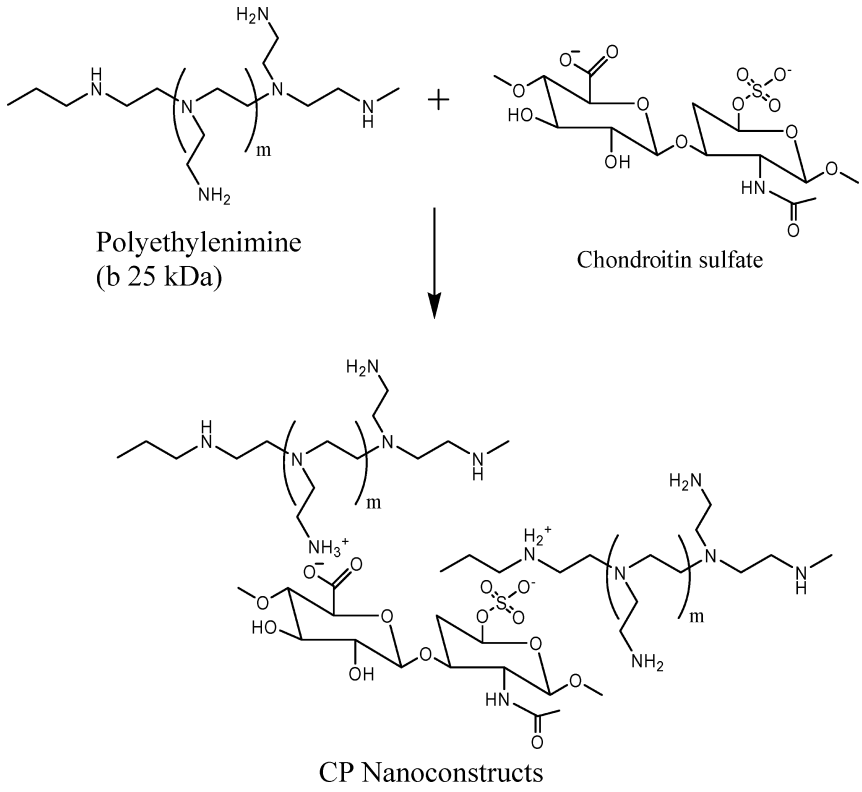

Scheme 1. Preparation of CP nanoconstructs.

concerns, nonionic and hydrophilic polymer, *viz.*, poly(ethylene glycol) (PEG), has been used to modify the surface of polyplexes.[12−16] Polysaccharide coating is considered to be a good alternative to PEGylation. The polysaccharide coat confers physicochemical stability to nanoconstructs in harsh environments and also endows them target-specificity.[17−21]

Chondroitin sulfate (CS) is a sulfated glycosaminoglycan (GAG) composed of a chain of alternating sugars (*N*-acetylgalactosamine and glucuronic acid). It is usually found attached to proteins as a part of proteoglycan.[22,23] CS is also a vital component in swelling and hydration of collagen fibril framework, intracellular signaling, cell orientation, and recognition and connection between extracellular matrix and cells.[24] Moreover, a receptor for CS, CD44, is known to be specifically overexpressed on various tumor cells,[25] and the affinity of CS to this receptor makes it an ideal candidate for site-specific drug delivery to solid tumors.

In the present investigation, we have explored the potential of CS−PEI (CP) nanoconstructs for tumor-specific gene delivery. The nanoconstructs were engineered by varying the content of CS. Additionally, nanoconstructs were characterized for physiochemical properties such as particle size, ζ-potential, morphology, and cytotoxicity to HepG2 and HeLa cells. The samples were almost nontoxic even at higher concentration. The CP nanoconstructs efficiently delivered pDNA *in vitro* in various cell lines and target Ehrlich ascites tumor (EAT) in mice.

RESULTS AND DISCUSSION

Synthesis of CP Nanoconstructs. Recent progress in bioengineering and nanotechnology that has given new insights into the cellular internalization pathways and DNA trafficking and a variety of nonviral gene carriers (*i.e.*, PEI, PLL, PAMAM, lipids, *etc.*) have been suggested for efficient transfer of pDNA. Among polycations, PEI, with its excellent proton sponge property, is the best studied carrier, and several attempts have been made to mitigate its charge-associated toxicity by modifications with diverse chemical moieties (*i.e.*, proteins, pegylation, acylation, polysaccharides, *etc.*).[17,26−28] We have embarked on the design, synthesis, and evaluation of application of CP nanoconstructs for targeting to solid tumor. The anionic polysaccharide CS interacted electrostatically with branched PEI (25 kDa) in aqueous solution under a controlled environment to form distinct and stable nanoconstructs. It is known that the polysaccharide coating on polycations increases the internalization of DNA in the cells and protects against intracellular enzymatic degradation.[29] The method of synthesis

TABLE 1. Particle Size and ζ-Potential Measurements of CP Nanoconstructs[a]

S. No.	nanoconstructs formulations	pDNA:nanoconstruct weight ratio	average particle size in nm (PDI)			ζ-potential (mV)		
			DNA loaded nanoconstructs (in cell culture media)	DNA loaded nanoconstructs (in H_2O)	nanoconstructs (in H_2O)	DNA loaded nanoconstructs (in cell culture media)	DNA loaded nanoconstructs (in H_2O)	nanoconstructs (in H_2O)
1	PEI 25 kDa	1:1	191 ± 2.11 (0.65)	399 ± 6.43 (0.40)	−	−	+38.1 ± 5.14	+44.2 ± 5.67
2	CP-1	1:10	77 ± 3.05 (0.48)	186 ± 4.87 (0.34)	92 ± 5.26 (0.17)	−25.3 ± 1.72	+23.2 ± 3.89	+37.8 ± 5.20
3	CP-2	1:10	93 ± 2.38 (0.46)	212 ± 5.27 (0.46)	124 ± 5.61(0.22)	−19.8 ± 1.54	+19.8 ± 3.12	+31.5 ± 4.63
4	CP-3	1:10	114 ± 3.65 (0.51)	276 ± 5.74 (0.48)	158 ± 6.57(0.11)	−17.6 ± 1.38	+16.4 ± 3.35	+25.4 ± 4.23
5	CP-4	1:10	131 ± 482 (0.22)	308 ± 5.58 (0.49)	174 ± 7.14(0.22)	−13.4 ± 1.11	+12.9 ± 2.22	+19.7 ± 3.45
6	CP-5	1:10	147 ± 4.26 (0.46)	352 ± 6.08 (0.51)	207 ± 7.36(0.46)	−9.1 ± 0.91	+9.3 ± 2.27	+12.3 ± 2.81

[a]The w/w ratio was selected at which the best transfection efficiency was obtained.

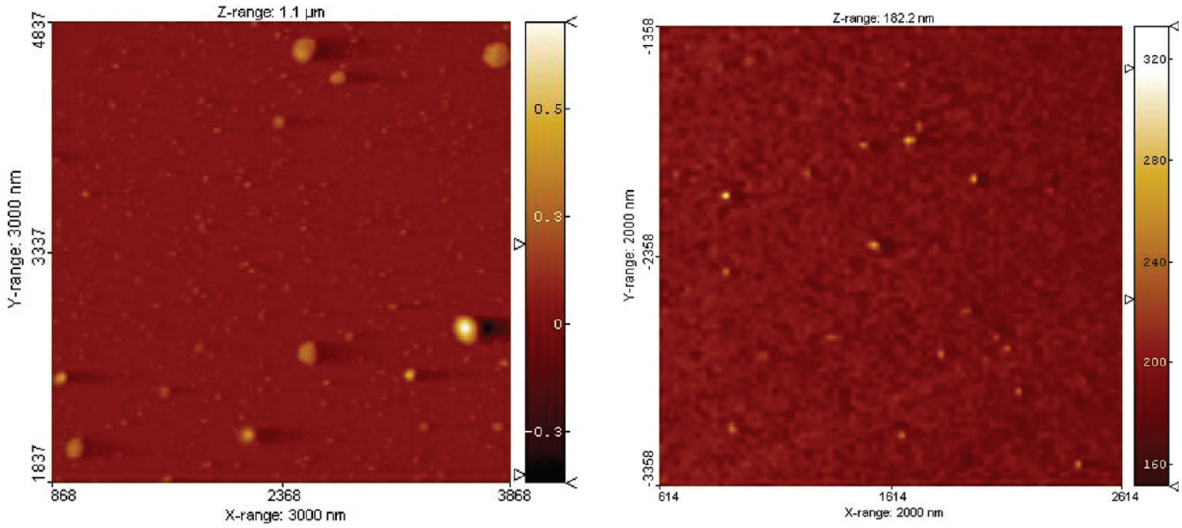

Figure 1. Atomic force microscopy images of CP-3 nanoconstruct. The 2−3 μL of each formulation was deposited on a freshly split untreated mica strip, and images were recorded in acoustic mode. (A) CP-3 nanoconstructs; (B) DNA/CP-3 nanoconstructs.

of CP nanoconstructs being straightforward, even a nonchemist can effortlessly synthesize these nanoconstructs. Chondroitin sulfate (CS), an anionic sulfated glycosaminoglycan, possesses high affinity toward CD44 receptors[30] and partially blocks the charge on PEI through electrostatic interaction (Scheme 1). Therefore, it was necessary to estimate the amount of sugar present in the nanoconstructs, which was done colorimetrically by the phenol-sulfuric acid method. The absorbance at 490 nm is proportional to the carbohydrate concentration present in a given sample. The percent of amino groups blocked in PEI by chondroitin sulfate was found to be 0.72% (1%), 1.48% (2%), 2.3% (3%), 3.1% (4%), and 3.9% (5%) in CP nanoconstructs (values in parentheses are the attempted percent of amino groups blocked with CS). The chondroitin sulfate incorporation in the nanoconstructs was ~70% of the attempted value. These nanoconstructs were further characterized by FTIR, and the bands at 3436 (amino stretching), 2850 and 1635 (carbonyl stretching), and 800−820 cm^{-1} (C−O−S stretching) clearly demonstrated the formation of CP nanoconstructs.

Particle Characteristics. The size and surface charge of gene carriers modulate their cellular uptake. A positively charged complex could interact with the negatively charged proteoglycans of the cell membrane. Dynamic light scattering experiments revealed that CP nanoconstructs formed compact particles averaging less than ~210 nm with polydispersity index lower than 0.450. As the concentration of chondroitin sulfate in the formulations increased, the ζ-potential decreased and the size of nanoconstructs was found to be increased (Table 1), which perhaps is due to electrostatic interactions of the amino group of PEI with the anionic sulfate moiety of CS. The particle size distribution pattern indicated that all particles were of nanometer size

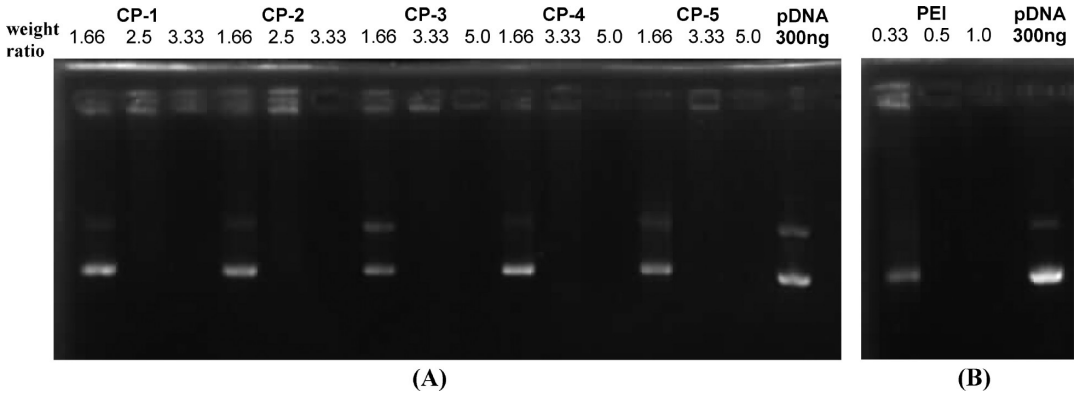

Figure 2. Gel retardation assay of (A) pDNA/CP nanoplexes and (B) pDNA/PEI complexes. The pDNA (300 ng) was incubated with increasing amount of nanoconstructs in 5% dextrose and incubated for 30 min. Samples were electrophoresed on a 0.8% agarose gel at 100 V for 60 min. The values mentioned correspond to the w/w ratio of pDNA/CP nanoplexes used in a 20 μL reaction. Sample size $n = 3$.

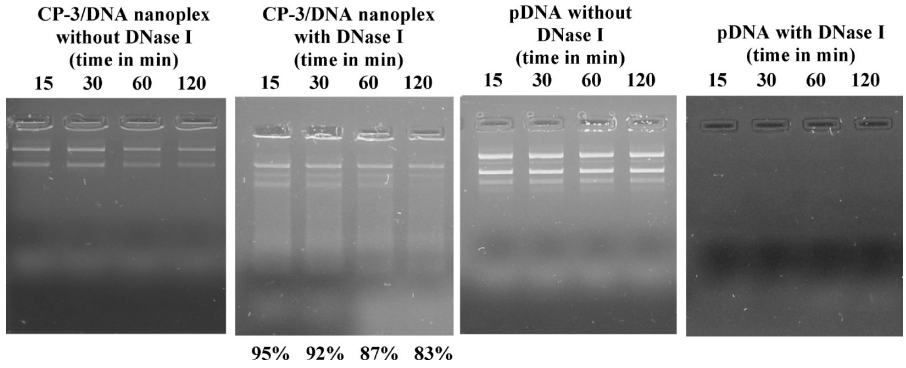

Figure 3. DNase protection assay. The pDNA (0.3 μg) alone and complexed with CP-3 nanoconstruct were exposed to PBS alone and DNase digestion. Samples were incubated at 37 °C and withdrawn after 15, 30, 60, and 120 min. The experiment was repeated three times.

and devoid of aggregates. On addition of DNA, size of nanoconstructs increased. The observed effect might be due to the wrapping up of pDNA around the surface of the nanoconstructs, forming a new outer layer, which led to an increase in the size of the CP nanoconstruct−DNA complex. The particle size and surface charge of nanoconstructs alone as well as DNA loaded were also recorded in the presence of transfection medium. As expected, the size reduced and the surface charge was negative in the presence of transfection medium (Table 1), which supports previous reports.[28,31] The average size of CP-3 nanoconstructs was found to be ~132 nm by AFM (Figure 1) and ~158 nm by DLS, and the difference in these values may be due to the hydrodynamic diameter recorded in the latter method. Under microscope, the nanoconstructs, alone as well as those loaded with DNA, were spherical in shape.

Retardation Assay. Gel retardation assay is widely utilized to monitor electrostatic interactions between cationic nanoconstructs and the anionic phosphate group of DNA backbone, and it also allows estimation of the most favorable polycation:pDNA ratio required to generate neutral complexes that cannot migrate during agarose gel electrophoresis.

CP nanoconstructs, prepared at different weight ratios, were incubated with a fixed amount of pDNA (0.3 μg) to determine the optimal concentration of nanoconstructs required for complete condensation of pDNA. The complexes were loaded into individual wells of 0.8% agarose/1× TAE gel in 0.5 μg/mL ethidium bromide and electrophoresed (100 V, 60 min). DNA and the nanoconstructs alone, diluted with the same buffer, served as controls (Figure 2). In case of PEI, retardation was observed at a weight ratio of 0.5:1 (PEI to pDNA), whereas a higher amount of CP nanoconstructs was needed to neutralize the same amount of pDNA. CP-1 and CP-2 nanoconstructs completely neutralized the pDNA at a weight ratio of 2.5:1. In the rest of the series, the amount of 1.0 μg of CP nanoconstructs was required to completely neutralize 0.3 μg of pDNA (weight ratio 3.33:1), indicating that the degree of chondroitin substitution slightly affects the pDNA complexing property of CP nanoconstructs. Results obtained from agarose gel electrophoresis are in full agreement with ζ-potential measurements. These results also confirmed that CS will not get displaced by competing anionic pDNA.

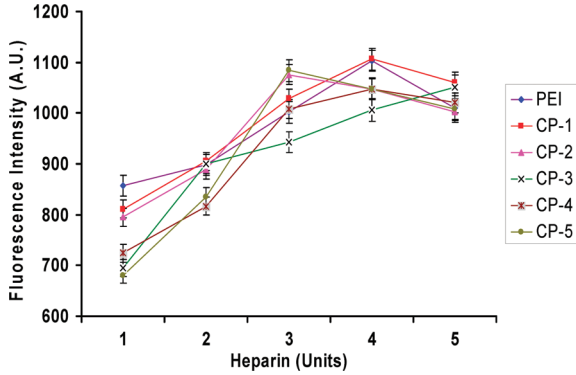

Figure 4. DNA release assay. The pDNA (0.3 μg) was mixed with EtBr (1 μg/mL) and the fluorescence recorded. Subsequently, to displace the pDNA from pDNA/CP nanoplexes, anionic polysaccharide, heparin, was added to each sample, allowed to incubate for 60 min, and measured the fluorescence intensity (arb unit). The values are expressed as the fluorescence signal intensity when ethidium bromide was bound to DNA, decreasing the competition from CP nanoconstruct (error bars represent ± standard deviation from the mean of three experiments).

Protection Assay. DNase I is an endonuclease enzyme that catalyzes the hydrolytic cleavage of phosphodiester linkages in the DNA backbone. The vulnerability of pDNA toward DNase I is one principal obstacle for the delivery of pDNA *in vitro* or *in vivo*.[31] In order to substantiate that the synthesized CP nanoconstructs provide protection to pDNA from nuclease, DNase I (as a model

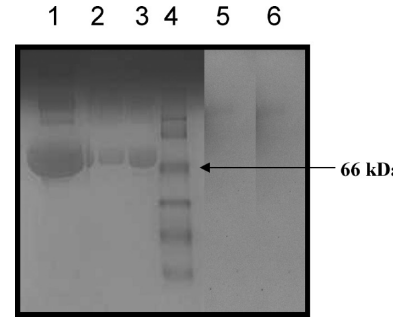

Figure 5. Protein adsorption onto surface of CP-3 nanoconstruct compared to adsorption onto native PEI. Lane 1 shows only BSA. Native PEI and CP-3 nanoconstruct incubated with BSA for 3 h are shown in lanes 2 and 3, respectively. Unbound BSA was removed by washing and centrifugation. Bound BSA was removed from the particles and run on a SDS−PAGE. Lane 4 represents the ladder. Native PEI and CP-3 nanoconstructs were also run without incubation with BSA in lanes 5 and 6, respectively.

enzyme) protection assay was carried out and analyzed by 0.8% agarose gel electrophoresis. The findings from the DNase I stability experiment are illustrated in Figure 3. Naked pDNA (0.3 μg) was degraded in 15 min after incubation with DNase I, while pDNA showed no significant degradation when complexed with CP-3 nanoconstruct (~17% after 2 h). This reveals that, under the physiological condition where the presence of nucleases significantly affects the integrity of pDNA, such formulations provide protection to pDNA. This demonstrates that the CP-3 nanoconstruct protects the pDNA effectively and is suitable for *in vivo* conditions.

pDNA Release and pDNA Loading Assay. The complexation of CP nanoconstructs with pDNA was examined by ethidium bromide intercalation assay. Ethidium bromide intercalates between the base pairs of DNA double helix, emitting an intense fluorescence signal at 610 nm when excited at 506 nm. When CP nanoconstructs were added to a solution containing ethidium bromide and pDNA, nanoparticles formed complexes with pDNA and displaced EtBr, which resulted in a decrease in fluorescence intensity. Further, addition of a competitor anionic molecule, heparin, caused DNA release from the complexes (Figure 4). On increasing the concentration of heparin, increased amount of DNA released and finally reached to a point at saturation level (Figure 4). The amount of heparin needed to release DNA from the nanoplexes was observed to be small when compared to DNA release from native PEI. The results indicate that the CP/DNA nanoplexes were neither too tightly nor too loosely bound. This result has a very important implication in release of the complexed pDNA in the cells. Nanoconstructs prepared were found to incorporate ~92% of pDNA.

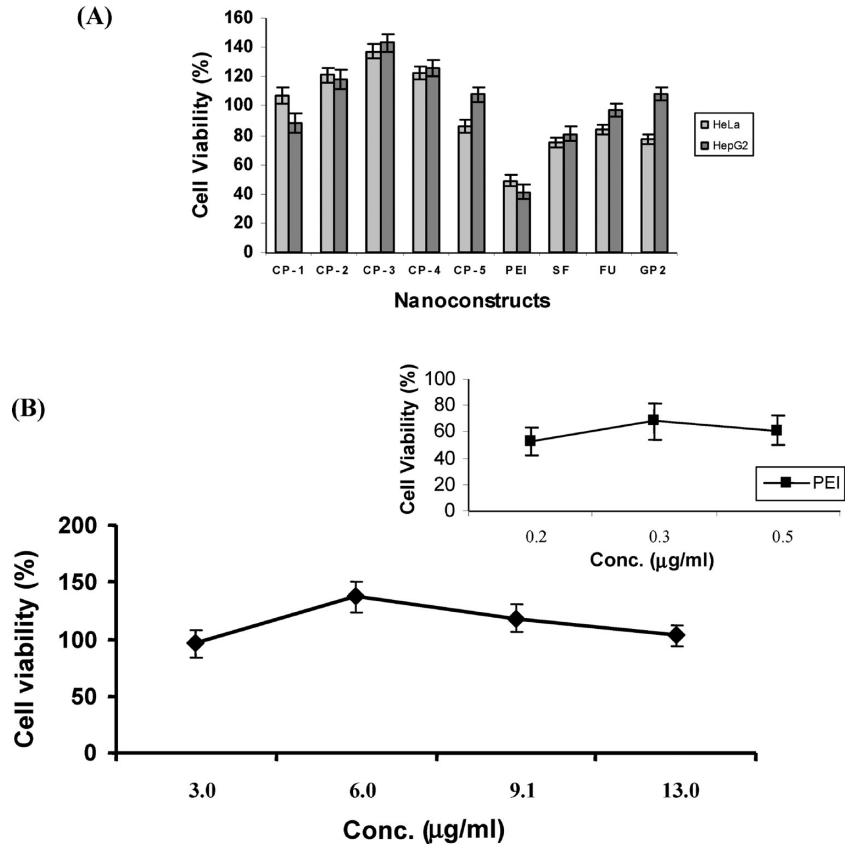

Figure 6. Cytotoxicity of pDNA/CP nanoplexes (1:10) and pDNA/PEI (1:1) complexes in HeLa and HepG2 cells. Cells were treated with pDNA/PEI complexes and pDNA/CP nanoplexes under conditions described in the Methods, and cytotoxicity was determined by MTT cell culture assay. Percent viability of cells is expressed relative to control cells. Each point represents the mean of three independent experiments performed in duplicate. (A) pDNA/CP nanoplexes (1:10), pDNA/PEI (1:1), superfect, fugene, and GenePORTER 2 complexes (following manufacturers' protocols) mediated cytotoxicity at various concentrations in HeLa and HepG2 cells. (B) Dose dependence curve for cytotoxicity mediated by pDNA/PEI and pDNA/CP-3 nanoplexes; 300 ng of pDNA was used (error bars represent ± standard deviation from the mean of the three experiments).

Protein Adsorption. Under *in vivo* conditions, adsorption of serum proteins is known to reduce transfection efficiency of the complexed pDNA.[31] In order to investigate the protein adsorption onto the exterior of CP-3 nanoconstruct, the system was incubated with BSA for 3 h. Free BSA was washed off, and the nanoconstruct was recovered by centrifugation. BSA bound to the exterior of the nanoconstructs was removed using SDS and separated from the system using SDS−PAGE. The amount of BSA adsorbed onto CP-3 nanoconstruct was compared with the amount of BSA adsorbed onto PEI (25 kDa). As depicted in Figure 5, the band of BSA removed from PEI after BSA incubation is much more intense than the band of BSA from the CP-3 nanoconstruct. The results indicate that CP-3 nanoconstruct adsorbed less protein than PEI and further bolster the fact that the polysaccharide coating could reduce the nonspecific binding of proteins, which was confirmed by the protein adsorption experiment.

Cell Metabolic Activity. The surfeit of positive charge on the polycationic polymers has been the key factor in their cellular toxicity. As revealed by a comparative study between cationic, neutral, and anionic polymers, the cationic polymers were found to destabilize and ultimately rupture the cell membrane due to strong electrostatic interaction. It was considered necessary to exemplify that the synthesized CP nanoconstructs were safe and did not harm the cells during the internalization process and efficiently express the gene intracellularly. In this study, the cell viability of CP nanoconstructs, PEI, superfect, fugene, and GenePORTER 2 was examined at various concentrations in HeLa and HepG2 cells (Figure 6). This demonstrates that cell toxicity is strongly dependent on substitution of CS on PEI. The results indicate that cell viability increased with increase

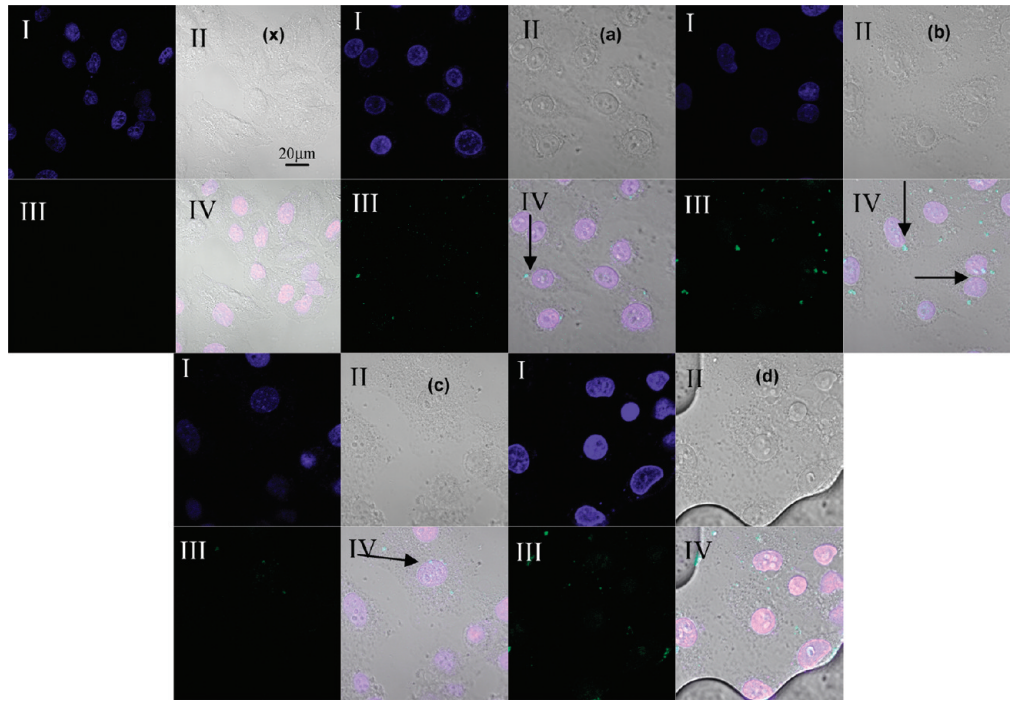

Figure 7. Confocal microscopic images of HeLa cells treated with fluorescein-labeled CP-3 nanoconstruct at different time points: (x) control (untreated cells) (a) 30 min, (b) 1 h, (c) 2 h, (d) 3 h. Each image is divided into four quadrants. Quandrant I, cells observed under DAPI filter; Quadrant II, image captured under bright field; Quadrant III, cells visualized under fluorescein filter; Quadrant IV, overlaid images. Arrows represent the location of the labeled CP-3 nanoconstruct inside the cell.

in substitution of CS in the nanoconstructs, and the average cell viability for CP-3 formulation (the best working system) was found to be >130%, whereas only ~45% cells was found to be viable in the case of PEI (25 kDa) in both the cell lines. This may be explained in terms of relatively higher hydrophilicity of the surface of CP nanoconstructs, which may prevent polymer aggregation and nonspecific adhesion to the cell surface, resulting in lower cytotoxicity.[33] The prominent feature of CP nanoconstructs is that, even beyond the best transfection efficiency achieved at a weight ratio of 1:10, the toxicity was not observed in the samples. It was also evident from Figure 6B (dose dependence curve) that cell viability of CP-3 nanoconstruct initially increased from the concentration of 3 μg/mL and acquired highest cell viability at 6 μg/mL. Beyond this concentration, the cell viability started decreasing. Our findings were in tune with the earlier reports[17,27,34] already published from the author's laboratory. The cell cytotoxicity results show considerable promise for the prospects of CP nanoconstructs in clinical applications.

Confocal Microscopy. The intracellular route of CP-3 nanoconstruct was determined by confocal imaging of a fluorescent-labeled nanoconstruct. For this purpose, nanoconstructs were added to HeLa cells, and the path of the labeled nanoconstructs was monitored at various time points (Figure 7). After 30 min of treatment of cells with labeled nanoconstruct, there was a faint fluorescence distributed homogeneously throughout the cell membrane. The fluorescence was distributed uniformly in the cytoplasm 1 h post-treatment with labeled CP-3 nanoconstruct. After 2 h, discrete patches of fluorescence were observed in the nucleus of the treated cells, which were retained inside the nucleus even after 3 h of treatment, which is an essential parameter for efficient transfection. The finding of nuclear localization of CP-3 nanoconstruct is consistent with the work that shows labeled PEI being transported into cell nuclei.[35]

***In Vitro* Gene Transfection.** Transfection experiments were performed on HEK293, HEK293T, HepG2, and HeLa cells using a plasmid containing reporter gene encoding green fluorescence protein (GFP). The weight ratio, higher than the ratio at which complete DNA retardation was observed, was used for transfection. The cells were exposed with various formulations of pDNA/nanoconstructs in 5% dextrose for 3 h. The cells were examined under the fluorescent microscope after 36 h. The transfected cells had a fairly high level of reporter gene expression and appeared to be healthy on microscopic examination (Figure 8A). The protein expression was quantified spectrofluorometrically at an excitation wavelength at 488 nm and emission wavelength of 509 nm. In the case of HEK293 cells, transfection efficiency of nanoconstructs was found to be improved ~1.5−5-fold compared to PEI (25 kDa) and superfect, fugene, and GenePORTER 2, which was found to increase in a dose-dependent manner, and the highest transfection was recorded with CP-3 formulation in all the cells. The dose dependence curve for transfection efficiency is

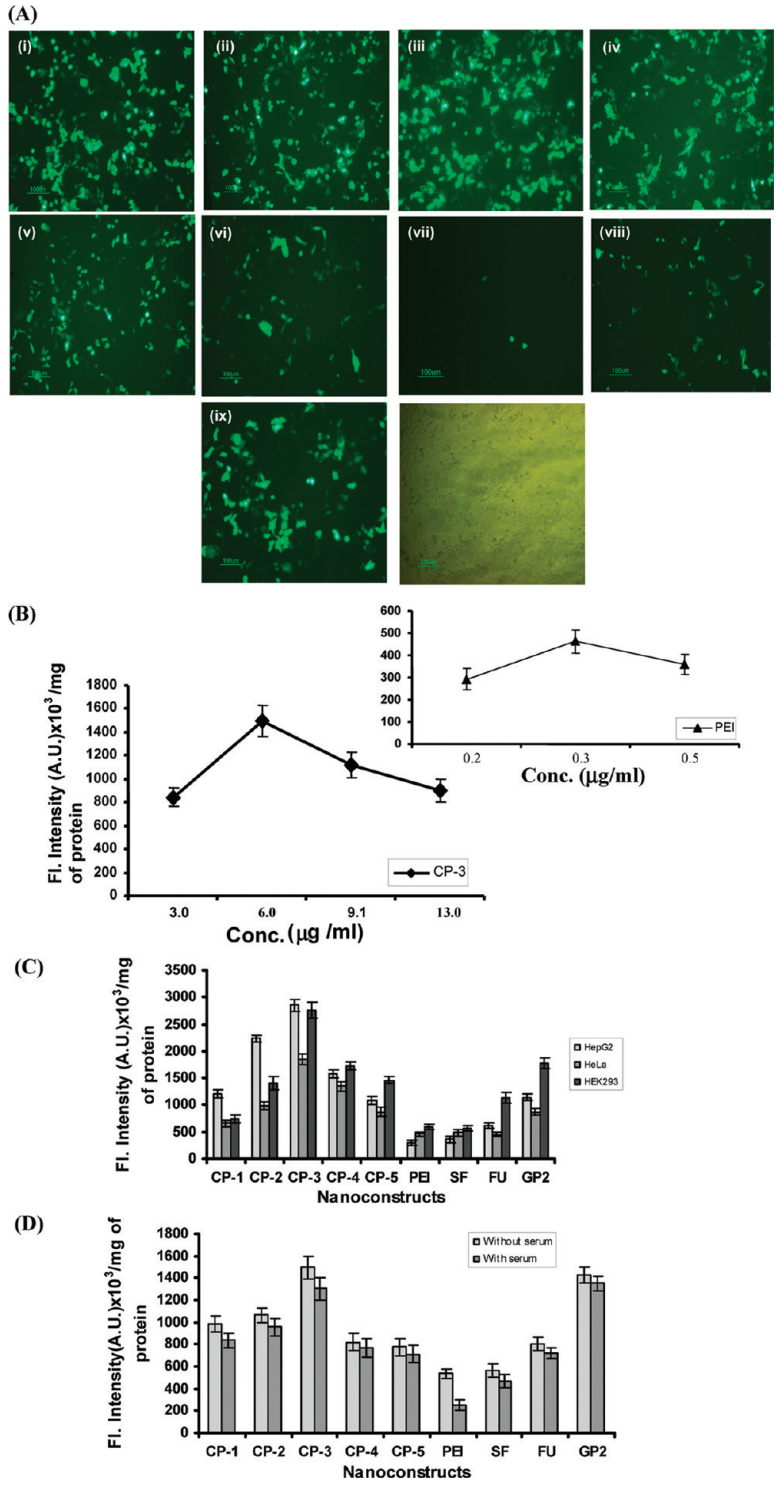

Figure 8. (A) GFP fluorescence images of HEK293 cells transfected with pDNA/CP, pDNA/PEI, superfect, fugene, and GenePORTER 2 complexes. HEK293 cells were incubated with pDNA/CP nanoplexes, pDNA/PEI, superfect, fugene, and GenePORTER 2 complexes for 3 h, and the expression of GFP was monitored after 36 h. The fluorescent intensity of GFP fluorophore in the cell lysate was measured on spectrofluorometer, and the results are expressed in terms of arbitrary units/mg total cellular protein. The results represent the mean of two independent experiments performed in triplicate. (i) CP-1 (1:10), (ii) CP-2 (1:10), (iii) CP-3 (1:10), (iv) CP-4 (1:10), (v) CP-5 (1:10), (vi) superfect, (vii) fugene, (viii) GenePORTER 2, (ix) PEI (1:1), (x) untreated cells, images were recorded at 10× magnification. (B) Fluorescent intensity of GFP fluorophore in the cell lysate was measured using spectrofluorometer, and the results are expressed in terms of arb unit/mg total cellular protein. The results represent the mean of two independent experiments performed in triplicate. Transfection efficiency with pDNA/PEI (inset) and DNA/CP-3 complexes prepared at various weight ratios. The abscissa represent the concentrations (μg/mL) of nanoconstructs used to condense 300 ng pDNA. The concentrations of unmodified PEI used were 0.2, 0.3, and 0.5 μg to condense 300 ng pDNA. (C) Transfection efficiency achieved by pDNA/CP nanoplexes in HeLa, HepG2m and HEK293 cell lines. (D) Maximum transfection achieved by pDNA/CP complexes in HEK293 cell lines (in presence and absence of serum) (error bars represent ± standard deviation from the mean); $n = 3$.

TABLE 2. Biodistribution Profile of pDNA/PEI and pDNA/CP-3 Nanoplex Formulations Labeled with ^{99m}Tc Following Intravenous Injection in Mice

	% dose recovered per gram of tissue after			
organ/tissue	1 h	3 h	6 h	24 h
pDNA/PEI complex				
blood	5.17 ± 1.21	3.15 ± 1.3	2.36 ± 0.98	0.32 ± 0.76
heart	0.55 ± 0.13	0.45 ± 0.11	0.34 ± 0.07	0.11 ± 0.03
lung	12.63 ± 1.41	9.21 ± 1.12	7.62 ± 1.05	1.83 ± 0.32
liver	35.47 ± 2.92	32.58 ± 2.76	28.64 ± 2.51	13.84 ± 1.48
spleen	32.54 ± 2.13	29.05 ± 2.03	27.84 ± 2.02	4.85 ± 0.78
kidney	12.59 ± 0.85	12.12 ± 0.81	8.95 ± 0.68	1.57 ± 0.11
stomach	0.65 ± 0.07	0.45 ± 0.06	0.42 ± 0.07	0.29 ± 0.05
intestine	0.35 ± 0.05	0.42 ± 0.07	0.46 ± 0.08	0.56 ± 0.07
muscle	0.21 ± 0.04	0.36 ± 0.05	0.38 ± 0.06	0.11 ± 0.02
tumor	0.23 ± 0.05	0.34 ± 0.04	0.41 ± 0.07	0.15 ± 0.03
tumor/muscle ratio	*1.10*	*0.94*	*1.08*	*1.36*
pDNA/CP-3 nanoplex				
blood	2.47 ± 0.51	1.99 ± 0.28	1.81 ± 0.21	0.84 ± 0.11
heart	0.37 ± 0.08	0.15 ± 0.03	0.16 ± 0.06	0.49 ± 0.09
lung	14.51 ± 1.39	10.2 ± 1.25	8.84 ± 0.94	23.9 ± 1.01
liver	33.69 ± 3.04	19.20 ± 2.91	25.35 ± 1.84	21.3 ± 0.88
spleen	30.40 ± 3.05	27.54 ± 3.78	29.70 ± 2.46	22.46 ± 0.81
kidney	9.8 ± 0.94	9.32 ± 0.87	6.1 ± 0.73	2.8 ± 0.32
stomach	0.94 ± 0.11	3.12 ± 0.08	2.4 ± 0.06	0.73 ± 0.03
intestine	0.51 ± 0.06	0.70 ± 0.05	0.66 ± 0.08	0.40 ± 0.11
muscle	0.9 ± 0.03	0.42 ± 0.07	0.37 ± 0.04	0.03 ± 0.05
tumor	1.025 ± 0.81	1.52 ± 0.18	1.96 ± 0.56	1.17 ± 0.37
tumor/muscle ratio	*1.12*	*3.62*	*5.29*	*13.01*

presented in Figure 8B,C. In HepG2 and HeLa cells also, the CP-3 formulation gave the maximum expression, which was found to be ~9- and 4-fold, respectively, as compared to PEI (Figure 8D). Weight ratios resulting in optimal transfection were also higher in the case of CP nanoconstructs compared to native PEI, which were well tolerated by the cells. As revealed in Figure 8C, maximum transfection efficiency was recorded in the case of CP-3 nanoconstruct at a pDNA/nanoconstructs ratio of 1:10, which was found to be ~6.5−1-fold higher than the PEI (25 kDa), superfect, fugene, and GenePORTER 2 on various cell types. It was observed that, on increasing the sugar content, the transfection efficiency increased and maximum transfection was obtained at CS substitution (2.3%), thereafter the gene expression started decreasing (Figure 8). CP nanoconstructs were also found to be efficient in the presence of serum (Figure 8D). The modified systems were found to be far superior in terms of toxicity issues and transfection efficiency on various cell types, as compared to the native PEI and the standard transfection reagents (Figure 8D,E). The superiority of the projected nanoconstructs in terms of toxicity and transfection efficiency to other vectors might be due to polysaccharide conjugation, which is considered to be a better option as these molecules provide hydrophilic environment to the conjugates, which prevent polymer aggregation and nonspecific adhesion to cell surface. Additionally, cells have been found to proliferate in the presence of carbohydrate moieties. Therefore, cell viability of CP nanoconstructs was found to be much higher as compared to native PEI and other vectors, which ultimately resulted in higher transfection efficiency.

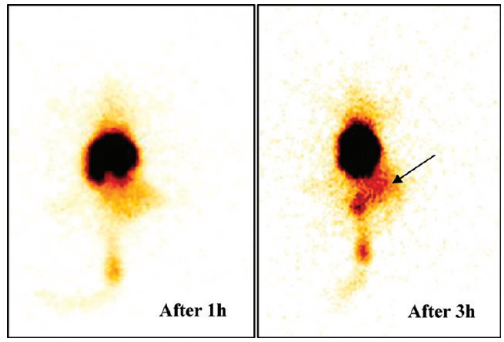

Figure 9. Gamma scintigraphic images of pDNA/CP-3 nanoplex treated tumor induced mice. Arrow represents accumulation of labeled CP-3 nanoconstruct at the tumor site.

Hematological Studies. The hematological study was undertaken to assess the toxic effect of CP-3 nanoconstruct on various blood parameters. In order to examine the safety of the nanoconstruct as a gene carrier, subacute toxicity was evaluated *in vivo* after repeated injection through the ear vein of rabbits for 7 days. Serum concentration of creatinine, blood urea nitrogen (BUN), aspartate transferase (GOT), and alanine transferase

(GPT) was found to be normal in all groups, indicating that the liver and renal functions were normal. All hematological parameters were also found to be normal in pDNA/CP-3 nanoplex treated animals. This means that the nanoconstruct formulation does not cause unexpected side effects and they are safe gene carriers (data not shown).

Radiolabeling, Biodistribution, and Scintigraphy Studies. The sodium pertechnetate ($^{99m}TcO_4^-$) was employed for radiolabeling of formulations. The amount of stannous chloride (reducing agent) employed for labeling plays an important role in determining labeling efficiency. A high amount of stannous chloride leads to the formation of radiocolloids (reduced/hydrolyzed $^{99m}TcO_4^-$), which is undesirable. On the other hand, lesser amounts of stannous chloride resulted in inferior labeling.[36−38] It was observed that, in all formulations, 80 μg of stannous chloride resulted in maximum labeling efficiency with minimum amount of free $^{99m}TcO_4^-$ (data not shown). The *in vitro* stability of the labeled formulations was assessed in PBS (pH 7.4). All formulations displayed high *in vitro* stability (data not shown). The formulations were >95% stable even after 24 h.

In order to evaluate the potential significance of the formulations, the biodistribution study was performed using ^{99m}Tc-labeled pDNA/CP-3 nanoplex and pDNA/PEI complexes. These experiments were performed in EAT-bearing mice models. The percentage dose per gram of tissue in different organs at different time intervals for pDNA/PEI and pDNA/CP-3 nanoplex is shown in Table 2. Further, it was found that pDNA/PEI cleared rapidly from the circulation. This may be attributed to very short biological half-life.[39] The sample was excreted through kidney, leading to very high activity in kidney (12.59 ± 0.85% ID/g tissue after 1 h, 12.12 ± 0.81% ID/g tissue after 3 h, 8.95 ± 0.68% ID/g tissue after 6 h, and 1.57 ± 0.11% ID/g tissue after 24 h). Relatively low concentration of pDNA/PEI complex was found in solid tumor, liver, and spleen after 24 h of administration. After 1 h of pDNA/PEI of administration, 33.69 ± 2.85 and 30.40 ± 2.24% ID/g tissue of radioactivity was found in liver and spleen, respectively, which decreases after 24 h (13.84 ± 1.48 and 4.85 ± 0.78% ID/g tissue in liver and spleen, respectively).

Again, CP-3 nanoconstruct appeared to rapidly clear from blood circulation in order to reach the target site (solid tumor), leading to significantly higher concentration of CP-3 formulation. The formulation was able to retain in these sites even post 24 h of administration (1.17 ± 0.37, 21.3 ± 0.88, and 22.46 ± 0.81% ID/g tissue was estimated in solid tumor, liver, and spleen, respectively). It is evident from the *in vivo* experiments that CS decorated PEI (CP-3 nanoconstruct) reaches the tumor mass in a significantly higher concentration in comparison to PEI, as shown by tumor to muscle ratio and gamma scintigraphic images in Table 2 and Figure 9, respectively. Results were found to be more pronounced even after 24 h of administration. Scintigraphic images of mice after administration of CP-3 nanoconstruct are shown in Figure 9. It was observed that sugar modification of the PEI appreciably enhanced its uptake by tumor cells after 3 h. This result attributed to the higher efficiency of nanoconstruct to accumulate within the tumor mass by virtue of the competition with endogenous and exogenous chondroitin sulfate in the tumor.[40−42] It has also been reported in the literature that malignant cells use CD44-related chondroitin sulfate proteoglycan as a matrix receptor to mediate migration and invasion. CD44 is a transmembrane glycoprotein with extracellular, membrane and cytoplasmic domains.[43] The extracellular domain of CD44 is capable of binding a variety of ECM molecules[44] and contains attachment sites for chondroitin sulfate.[44−48] The ascites cells exhibit an active production of sulfated mucopolysaccharides (*i.e.*, chondroitin sulfate, hyaluronic acid) predominantly at the mitochondria and cell membrane level.[42,49] Therefore, the results of iv administration of pDNA/CP-3 nanoplex exhibit the significance of this system in transfecting tumor mass. From the biodistribution studies, it was concluded that the residence time of pDNA/CP-3 nanoplex in the tumor mass was significantly higher as compared to the PEI (25 kDa). The longer residence time of the CP-3 nanoconstruct in the tumor mass suggests its potential for uptake into the cells.

CONCLUSIONS

Literature records numerous gene delivery systems. However, only a few of them successfully tested in clinical trials have shown promise. The reasons for failure to translate preclinical findings into clinical setting include inefficient gene delivery, toxicity, stability, and other factors related to scaling and manufacturing of gene delivery vehicle. The projected CP nanoconstructs show promising opportunities for the design of PEI-based gene delivery agents by blending with a biocompatible mucopolysaccharide (chondroitin sulfate) in appropriate ratio, which can efficiently deliver a pDNA into the mammalian cells. The blending of CS to PEI decreases its charge-associated cytotoxicity and thereby improves the transfection efficiency. Since our methodology for the preparation of nanoconstructs is simple and straightforward, findings reported here should facilitate both basic and clinical research employing CP nanoconstruct mediated gene delivery. The targeting ability of CS-modified nanoconstruct to solid tumor is supported by *in vivo* experiments. These findings cumulatively strengthen the expectation that CS-modified PEI-based nanoconstructs could symbolize a potential alternative to gene therapy of tumor.

METHODS

Cell Culture and Materials. The cells, HEK293 (human embryonic kidney), HEK293T (SV40 large T antigen contained in human embryonic kidney), HepG2 (human hepatocellular liver carcinoma), and HeLa (human cervical adenocarcinoma), were obtained from the cell repository facility of National Centre for Cell Sciences, Pune, India. For *in vitro* transfection, HEK293, HEK293T, HepG2, and HeLa cell lines were maintained 16 h before the experiments as monolayer cultures in Dulbecco's Modified Eagle's culture medium (DMEM) (GIBCO-BRL-Life Technologies, Web Scientific Ltd., UK) supplemented with 10% heat-inactivated fetal calf serum (FCS) (GIBCO-BRL Life Technologies) and 1% antibiotic (streptomycin + penicillin). Cultures were maintained at 37 °C in a humidified 5% CO_2 atmosphere.

PEI (25 kDa, branched), chondroitin sulfate, 3-(4,5-dimethylthiazol-2-yl)-2,5-diphenyltetrazolium bromide (MTT), agarose, Tris, HEPES, bromophenol blue (BPB), ethidium bromide (EtBr), xylene cyanol (XC), and high retention dialysis tubing (cut off 12 kDa) were obtained from Sigma-Aldrich Chemical Co., St. Louis, MO. Bradford reagent was purchased from Bio-Rad Inc. Standard transfection reagents superfect (PAMAM dendrimer), fugene (nonliposomal multicomponent reagent), and GenePORTER 2 (liposome) were purchased from Qiagen (Courtaboeuf, France), Roche Applied Science (Indianapolis, IN), and Gelantis (San Diego, CA), respectively. Sephadex G-20 columns were procured from GE Healthcare, USA. Plasmid purification kit was purchased from Qiagen (Courtaboeuf, France). Sodium pertechnetate freshly eluted from ^{99m}Mo by solvent extraction method was procured from Regional Centre for Radiopharmaceuticals (Northern Region), Board of Radiation and Isotope Technology (BRIT), Department of Atomic Energy, India. Strain A mice and female New Zealand rabbits were procured from the animal house of the Institute of Nuclear Medicine and Allied Sciences, Delhi, India. Stannous chloride (extrapure, BP grade) was purchased from Merck KgaA, Germany. Acetone (chromatography grade, Lichrosolv) and acetic acid (100% aldehyde free) were obtained from Merck, India. All chemicals, reagents, and solvents in the present experiment were of the highest grade available and used as directed. All the experiments were carried out using Milli-Q (deionized) water filtered through 0.22 μm sterile filters (Millipore).

Preparation of Plasmid DNA (pDNA). The plasmid encoding enhanced green fluorescent protein gene (EGFP) under the cytomegalovirus (CMV) immediate early promoter was constructed. The plasmid was propagated into competent *Escherichia coli* bacterial strain DH5a, and endotoxin-free preparation of plasmid was purified following alkaline lysis maxiprep columns (Qiagen S.A., Courtaboeuf, France) as per manufacturer's instructions. The purity and identity of the plasmid was confirmed by agarose gel electrophoresis and by the ratio of UV absorbance 260/280 in Milli-Q water.

Preparation and Characterization of CP Nanoconstructs. Chondroitin sulfate sodium salt (2.9 mg) was dissolved in dd water (25 mL), and dilute HCl (1 N, 5 mL) was added. After 30 min, the solution was concentrated and reconstituted in Milli-Q water (25 mL). Subsequently, it was added dropwise to a stirred solution of PEI (50 mg dissolved in 100 mL of water) with continuous stirring and left for stirring overnight. The reaction mixture was concentrated on a rotary evaporator and then lyophilized in a speed vac to obtain CP (1%) nanoconstructs in ~75% yield, as a white powder. Likewise, other CP nanoconstructs (2, 3, 4, and 5% of CS) were prepared by varying the amount of chondroitin sulfate. The sugar concentration in the nanoconstructs was determined by the phenol-sulfuric acid method.[50] Briefly, 25 μL of CP nanoconstructs (1 μg/μL) was mixed thoroughly with 15 μL of freshly prepared phenol solution (5% w/v) in dd water and 90 μL concentrated H_2SO_4 (95−97%). The mixture was incubated for 30 min at room temperature, diluted with dd water to 1.0 mL, and the absorbance was measured spectrophotometrically on a Perkin-Elmer Lambda Bio 20 UV−vis spectrophotometer at 490 nm. The sugar content in the nanoconstructs was calculated from a standard calibration curve drawn by taking known concentrations of CS. These nanoconstructs were further characterized by Fourier transform infrared (FTIR) spectroscopy. Spectra of the CP nanoconstructs were recorded on a single beam Perkin-Elmer (Spectrum BX Series), with the scan parameters: scan range, 4400−400 cm^{-1}; number of scans, 16; resolution, 4.0 cm^{-1}; interval, 1.0 cm^{-1}; unit, %T.

Shape, Size, and ζ-Potential Measurements. The hydrodynamic diameters and ζ-potential of nanoconstructs and nanoconstructs/DNA complexes were measured using Zetasizer Nano-ZS, Malvern Instruments (Worcestershire, UK) employing a nominal 5 mW HeNe laser operating at 633 nm wavelength with the following settings: 15 measurements per samples, viscosity for water is 0.89 cP, temperature 25 °C. DNA complexes were prepared by incubating the various concentrations of nanoconstructs and pDNA for 30 min at room temperature. The Smoluchowski approximation was used to calculate ζ-potential from the electrophoretic mobility. Further, the size and surface morphology of the nanoconstructs and DNA complexes were determined by atomic force microscopy, PicoSPM system (Molecular Imaging, AZ) operating in acoustic mode, using SPIP software, an image analyzing software for scanning probe microscopy. A 250 μm long magnetically coated cantilever (AAC lever) with a spring constant of 2.8 N/m and resonance frequency of ~65 kHz was used. Briefly, a solution (2−3 μL) of each nanoconstruct was deposited on a freshly split untreated mica strip and allowed to dry for 5 min at room temperature. Consequently, the mica surface was imaged. Particle size was obtained using SPIP software.

DNA Loading Efficiency. The quantity of pDNA bound to the CP-3 nanoconstruct was examined by measuring the difference between the total amount of pDNA electrostatically bound to the nanoconstruct and the amount of nonbound residual pDNA in the aqueous suspension after filtration through a Millipore Centricon YM-100 (100 kDa cutoff) membrane filter. The recovered complex was dissolved in water (2 mL) and subjected to lyophilization in a speed vac. Subsequently, a weighed amount of the sample (CP-3 nanoconstructs, 2 mg) was dissolved in Tris buffer (1 mL, 10 mM, pH 7.4) and filtered. The filtrate was analyzed for content of pDNA spectrophotometrically at 260 nm.

Gel Migration Assay of pDNA/CP Nanoplexes. The pDNA/CP nanoplexes prepared at different weight ratios in 5% dextrose were electrophoresed on 0.8% agarose gel for 60 min at 100 V. All the samples were incubated for 30 min at room temperature prior to loading on the agarose gel. The pDNA/CP nanoplexes were mixed with a tracking dye (xylene cyanol), total volume made to 20 μL, and loaded into individual wells, electrophoresed, stained with EtBr, and visualized on a UV transilluminator.

DNase Protection Assay of pDNA/CP Nanoplexes. In order to confirm the ability of CP nanoconstructs to protect the condensed pDNA from endonucleases, DNase I protection assay was executed as reported earlier.[51] The pDNA/CP nanoplexes and pDNA were incubated at 37 °C with 1 μL of DNase I (1000 units/ml) or in 1× PBS and withdrawn at different time intervals (15, 30, 60, and 120 min). The experiments were terminated by the addition of 5 μL of 0.1 M EDTA solution for 10 min to inactivate DNase, followed by incubation for 2 h with 10 μL of heparin (5 mg/mL) to completely dissociate polyplexes. A qualitative analysis of DNA degradation was performed by gel electrophoresis, as described above.

DNA Release Assay. The pDNA (20 μg/mL) was mixed with EtBr (1 μg/mL), and the fluorescence of the resulting complex was measured using Nanodrop ND 3300 spectrofluorometer (Thermo Fisher Scientific) having excitation at 506 nm and emission at 610 nm.[52] Background fluorescence was set to 0% using EtBr (1 μg/mL) solution alone. To allow complete displacement of the DNA from pDNA/CP nanoplexes, anionic polysaccharide, heparin, was added in small aliquots of 1 U (1 μL of 1 mg/195 μL solution) to each sample and incubated for 60 min. Results were expressed in terms of fluorescence intensity (arb unit) when ethidium bromide was bound to DNA in the absence of competitor.

Protein Adsorption Assay. The protein adsorption on native PEI (25 kDa) and CP-3 nanoconstructs was determined as reported earlier.[32] Briefly, PEI and CP-3 nanoconstructs were complexed with pDNA at a charge ratio of 1:0.5 and 1:10, respectively. Samples were incubated with standard bovine serum albumin (BSA, Bangalore Genei) for 3 h at room temperature. Final concentration of pDNA and BSA used was 3 μg/mL and 1 mg/mL, re-

spectively. The mixtures were centrifuged at 14 000*g* for 2 h at 4 °C. The supernatant was removed, and the pellet was washed with Milli-Q water to remove unbound BSA. The pellet was resuspended in loading buffer (0.2 M Tris-HCl pH 6.8, 10% w/v sodium dodecyl sulfate (SDS), 20% v/v glycerol, 0.05% w/v bromophenol blue, 10 mM dithiothreitol) (10 μL) and incubated at 100 °C for 5 min to extract bound BSA from the samples. Extracted solutions were loaded onto a 12% denaturing SDS−polyacrylamide gel and electrophoresed for 2 h at 25 mA. Thereafter, gel was stained with easy blue (Fermantas International Inc., Canada) stain to visualize BSA that had adsorbed onto PEI and CP-3 nanoconstructs.

Cell Cytotoxicity Assay. Cytotoxicity of the formulations was evaluated by 3-(4,5-dimethylthiazol-2-yl)-2,5-diphenyltetrazolium bromide (MTT) colorimetric assay in HepG2 and HeLa cells. HepG2 cells (12 000 cells/well) were seeded in 96-well cell culture plates and cultured in DMEM medium with 10% FCS overnight. Before the transfection experiment, medium was replaced with fresh DMEM with or without 10% FCS. PEI, CP nanoconstructs, superfect, fugene, and GenePORTER 2 were complexed with pDNA (total volume 20 μL) and added to each well followed by 3 h incubation at 37 °C in CO_2 incubator. Thereafter, transfection mixture was replaced by 100 μL of fresh DMEM containing 10% FCS, and cells were incubated for an additional 36 h. Likewise, experiments were carried on HeLa cells. After 36 h, medium was aspirated and 100 μL of MTT (0.5 mg in 1.0 mL of DMEM) was added to cells followed by incubation for 30 min at 37 °C. Thereafter, the supernatant was removed and the cells were rinsed with PBS. The formazan crystals formed were dissolved in 100 μL of isopropanol containing 0.006 M HCl and 0.5% SDS and absorbance of the solution was measured at 540 nm on an ELISA plate reader (MRX, Dynatech Laboratories). Untreated cells were taken as control with 100% viability, and cells without addition of MTT were used as blank to calibrate the spectrophotometer to zero absorbance. The relative cell viability (%) compared to control cells was calculated by $A_{sample}/A_{control} \times 100$.

Confocal Laser Scanning Microscopy Experiment. In order to elucidate the path of CP nanoconstructs inside the cells *in vitro*, HeLa cells was exposed to fluorescein-labeled CP-3 nanoconstruct.[34] Briefly, CP-3 nanoconstruct (10 mg/mL of water) was treated with fluorescein isothiocyanate (FITC) (1 mg/100 μL of DMF) overnight with stirring, followed by concentration in a speed vac. Unreacted/hydrolyzed FITC was extracted with ethyl acetate to obtain fluorescein-labeled CP-3 nanoconstruct. HeLa cells were grown in supplemented DMEM overnight to ~70% at a density of 100 000 cells per well on glass coverslips in six-well microplates. A suspension of fluorescein-labeled nanoconstruct was prepared at a concentration of 0.024 mg/mL in the culture medium. The nanoconstruct suspension was incubated with the HeLa cells at 37 °C for 15 min, 30 min, 1.0 h, 2.0 h, and 3.0 h. The medium was then aspirated out, and the plates were washed three times with sterile 1× PBS. At predetermined time intervals, the cells were fixed with 4% (v/v) paraformaldehyde in PBS for 10 min at room temperature and washed four times with PBS. Individual coverslips were stained with DAPI and then mounted on clean glass slides with fluorescence-free glycerol-based mounting medium (Fluoromount-G1; Southern Biotech Associates, Birmingham, AL). Differential interference contrast (DIC) and fluorescence images were acquired with a Zeiss 510 Meta confocal microscope (Axio Observer, Carl Zeiss MicroImaging GmbH, Germany).

***In Vitro* Transfection Efficiency.** HEK293 cells (12 000 cells/well) were seeded in 96-well cell culture plates and cultured in DMEM medium with 10% FCS overnight. Cells were treated similarly, as described in the cytotoxicity experiment. Likewise, experiments were carried on HEK293T, HepG2, and HeLa cells. Inverted fluorescent microscope (Nikon Eclipse 2000E, Kanagwa, Japan) fitted with C-F1 epifluorescence filter, Ex 450-490, dichroic mirror DM 505, and barrier filter BA 520 was used to visualize the cells expressing EGFP. Transfection experiments were repeated five times to demonstrate reproducibility of results.

EGFP Expression Analysis. The fluorescence intensity was measured to quantify the GFP expression in the mammalian cells. Cells in each well were washed with PBS (1 × 50 μL) and incubated with 100 μL of cell lysis buffer (10 mM Tris-HCl, pH 7.4, 0.5% SDS, and 1 mM EDTA). The cell lysates were collected, centrifuged to pellet the cellular debris, and 2 μL of cell lysate was used to estimate the GFP spectrofluorometrically at an excitation wavelength of 488 nm and emission at 509 nm. Background fluorescence and autofluorescence were determined using mock treated cells. The total recovered cellular protein content in cell lysate from each well was estimated using Bradford reagent by taking BSA as a standard. The amount of protein was estimated from a standard curve. The fluorescence intensity of GFP was calculated by subtracting the background values and normalized against protein concentration in cell extracts. The data are presented as arbitrary units (arb unit)/mg of cell protein, and results represent mean ± standard deviation for triplicate samples.

Hematological Study. Healthy, albino New Zealand rabbits having body weight between 2.5 and 3.5 kg with no prior drug treatment were employed for all the hematological/pathological studies. The rabbits were preserved on standard diet and water. All animal studies were carried out under the guidelines compiled by CPCSEA (Committee for the Purpose of Control and Supervision of Experiments on Animals, Ministry of Culture, Govt. of India), and all the study protocols were approved by Institutional Animal Ethics Committee. The animals were divided into two groups having three rabbits in each group. Blood samples were collected from all animals on day zero and analyzed for hemoglobin (Hb) content, RBC count, total leukocyte counts, and differential leukocyte counts in pathology lab. In addition, serum concentrations of blood urea nitrogen, creatinine, SGPT, and SGOT were also measured. First group of rabbits were administered a single intravenous dose of pDNA/CP-3 nanoplex daily for 7 continuous days followed by 7 days rest period. Second group was kept as control and given dose of normal saline instead of nanoconstructs. Blood samples were collected from the animals after 15 days and were analyzed for the same parameters as described above.

Radiolabeling of pDNA/PEI and pDNA/CP-3 Nanoplex. The pDNA/PEI and pDNA/CP-3 nanoplexes were labeled with ^{99m}Tc by direct labeling method using stannous chloride ($SnCl_2$) as a reducing agent. In brief, 100 μL of sodium pertechnetate ($^{99m}TcO_4^-$, approximately 2 mCi, obtained by solvent extraction method from molybdenum) was mixed with 50 μL of stannous chloride solution (defined concentration to give 25−200 μg of stannous chloride in 50 μL) in 10% acetic acid solution to reduce the technetium. The pH of the solution was adjusted to 6.5−7.0 using 0.5 M sodium bicarbonate solution. To this mixture was added a solution of pDNA/CP-3 nanoplex (1 mg/mL, 1 mL) and incubated for 15 min at room temperature. This procedure could also lead to the formation of radiocolloids (reduced and hydrolyzed ^{99m}Tc, TcO_2), which were separated and formulations were purified by Sephadex G-20 column (GE Healthcare, USA) using normal saline as an eluent. The fractions were collected, and radioactivity was measured in each fraction using a dose calibrator (CRC 15R, Capintec Inc., USA). Each fraction was further observed under an atomic force microscope (after decay of radioactivity) to determine the elution profile of nanoconstructs and radiocolloids in order to confirm the purity of labeled formulations. Likewise, pDNA/PEI was prepared and purified. The labeled formulations thus obtained were stored in sterile evacuated sealed vials for subsequent studies.

Labeling Efficiency and *In Vitro* Stability. Labeling efficiency of the purified radiolabeled formulations was determined by ascending instant thin layer chromatography (ITLC) using silica gel (SG)-coated fiber sheets of approximately 10 cm in length (Gelman Science Inc., Ann Arber, MI). The ITLC was performed using 100% acetone as the mobile phase. A tiny drop (2−3 μL) of the radiolabeled formulation was applied on the ITLC plate and allowed to run in acetone, and the solvent front was allowed to reach approximately 8 cm from the origin. The strip was cut into two equal halves, and the radioactivity in each segment was determined in a well-type γ-ray counter (γ-ray scintillation counter, type CRS 23C, Electronics Corporation of India Ltd., Mumbai, India). The free $^{99m}TcO_4^-$ moved with the solvent ($R_f = 0.9$), while the radiolabeled formulation remained at the point of application. Percent labeling efficiency was calculated from the follow-

ing formula: 100 − [$T \times 100$]/[$T + B$], where T and B are the counts at top and bottom, respectively.

For the determination of *in vitro* stability of the labeled formulations, 100 μL of the labeled formulation was mixed with 2.0 mL of PBS (pH 7.4) and incubated at room temperature, and change in labeling efficiency was monitored over a period of 24 h by ITLC as described above.

***In Vivo* Stability of the Labeled Complexes.** The experiment was performed in normal, healthy, female New Zealand rabbits weighing 2.5−3.5 kg. Animals were injected with about 500 μCi of ^{99m}Tc-labeled formulations through the dorsal ear vein. The blood was withdrawn through the vein of the other ear at different periodic intervals and spotted on the ITLC strips, which were developed as described previously to estimate the possible separation of free ^{99m}Tc/degradation of the complex under *in vivo* conditions.

Biodistribution and Scintigraphy Studies of ^{99m}Tc-Labeled PEI and CP-3 Nanoplex. The *in vivo* efficiency of CP-3 nanoconstruct to target solid tumor was examined in the Ehrlich ascites tumor (EAT) model. Strain A mice (aged 2−3 months) weighing between 25 and 30 g were selected for the experiments. The animals were provided food and water *ad libitum* and housed in an environment of controlled temperature and humidity. Prior to any experimentation, the animals were allowed to acclimatize in their new habitat for at least 48 h. Approximately 2.5×10^7 EAT cells were injected into the hind left flank region of the mice to inoculate tumors. Following tumor inoculation, the animals were monitored daily until subcutaneous tumors were palpable and ~15 mm in diameter.

The tumor-bearing mice were divided into two groups of six animals in each group. The first group of mice were injected with ^{99m}Tc-labeled pDNA (15 μg)/PEI (1.5 μg) complex through their tail vein; the second group of mice were injected with ^{99m}Tc-labeled pDNA (15 μg)/CP-3 nanoplex (10 μg) complex. After 1, 3, 6, and 24 h of injection, the mice were humanely sacrificed, and blood was collected by cardiac puncture, and organs (*e.g.*, heart, lungs, liver, spleen, kidney, stomach, intestine, muscle, and tumor) were excised and washed with Ringer solution to remove surface blood and adherent debris; radioactivity was measured using well-type γ-scintillation counter. The blood and organs were collected in preweighed tubes.

Scintigraphy (γ imaging) was performed in normal, healthy, strain A mice weighing 25−30 g using a γ camera (model SYS000002, Elgems Millenium, USA) autotuned to detect the 140 keV radiation of ^{99m}Tc. Mice were injected with ^{99m}Tc-labeled nanoconstructs through the tail vein and were anesthetized by intramuscular injection of 0.4 mL of ketamine at the time of imaging (50 mg/mL ketamine, Themis Chemicals, Mumbai, India). The mice were positioned under the γ camera after 1 and 3 h of administration of the formulations, and imaging was performed.

Acknowledgment. Financial grant from the CSIR Task Force Project (NWP035) is gratefully acknowledged. Authors are thankful to Dr. M. Ganguli, Dr. N. Singh, and Dr. G. W. Rembodkar for their help in AFM and CLSM experiments, respectively.

REFERENCES AND NOTES

1. Verma, I. M.; Somia, N. Gene Therapy: Promises, Problems and Prospects. *Nature.* **1997**, *389*, 239–242.
2. Piskin, E.; Dincer, S; Turk, M. Gene Delivery: Intelligent But Just at the Beginning. *J. Biomater. Sci., Polym. Ed.* **2004**, *15*, 1181–1202.
3. Górecki, D. C. Prospects and Problems of Gene Therapy: An Update. *Expert Opin. Emerg. Drugs* **2001**, *6*, 187–198.
4. Górecki, D. C. Gene Therapy: Prospects and Problems. *Expert Opin. Emerg. Drugs* **1999**, *4*, 247–261.
5. Luo, D.; Saltzman, W. M. Synthetic DNA Delivery Systems. *Nat. Biotechnol.* **2000**, *18*, 33–37.
6. Simoes, S.; Filipe, A.; Faneca, H.; Mano, M.; Penacho, N.; Duzgunes, N.; Limade, M. P. Cationic Liposomes for Gene Delivery. *Expert Opin. Drug Delivery* **2005**, *2*, 237–254.
7. Zhang, X; Godbey, W. T. Viral Vectors for Gene Delivery in Tissue Engineering. *Adv. Drug Delivery Rev.* **2006**, *58*, 515–534.
8. Curiel, D. T.; Agrawal, S.; Wagner, E.; Cotton, M. Adenovirus Enhancement of Transferrin-Polylysine-Mediated Gene Delivery. *Proc. Natl. Acd. Sci. U.S.A.* **1991**, *88*, 8850–8854.
9. Lemkine, G. F.; Demeneix, B. A. Poly(ethylenimine) for *In Vivo* Gene Delivery. *Curr. Opin. Mol. Ther.* **2001**, *3*, 178–182.
10. Godbey, W. T.; Wu, K. K.; Mikos, A. G. Poly(ethylenimine) and Its Role in Gene Delivery. *J. Controlled Release* **1999**, *60*, 149–160.
11. Behr, J.-P. The Proton Sponge: A Trick to Enter Cells the Viruses Did Not Exploit. *Chimia* **1997**, *51*, 34–36.
12. Katayose, S.; Kataoka, K. Water-Soluble Polyion Complex Associates of DNA and Poly(ethylene glycol)-Poly(L-lysine) Block Copolymer. *Bioconjugate Chem.* **1997**, *8*, 702–707.
13. Choi, Y. H.; Liu, F.; Kim, J. S.; Choi, Y. K.; Park, J. S.; Kim, S. W. Polyethylene Glycol-Grafted-Poly-L-lysine as Polymeric Gene Carrier. *J. Controlled Release* **1998**, *54*, 39–48.
14. Peracchia, M. T.; Vauthier, C.; Desmaele, D.; Gulik, A.; Dedieu, J. C.; Demoy, M.; d'Angelo, J.; Couvreur, P. PEGylated Nanoparticles from a Novel Methoxypolyethylene Glycol Cyanoacrylate-Hexadecyl Cyanoacrylate Amphiphilic Copolymer. *Pharm. Res.* **1998**, *15*, 550–556.
15. Kaul, G.; Amiji, M. Long-Circulating Poly(ethyleneglycol)-Modified Gelatin Nanoparticles for Intracellular Delivery. *Pharm. Res.* **2002**, *19*, 1061–1067.
16. Davis, F. F. The Origin of PEGnology. *Adv. Drug Delivery Rev.* **2002**, *54*, 457–458.
17. Patnaik, S.; Aggarwal, A.; Goel, A.; Ganguli, M.; Saini, N.; Singh, Y.; Gupta, K. C. PEI-Alginate Nanoconstrcts as Efficient *In Vitro* Gene Transfection Agents. *J. Controlled Release* **2006**, *114*, 398–409.
18. Rodrigues, S.; Santos-Magalhaes, N. S.; Coelho, L. C. B. B.; Couvreur, P.; Ponchel, G.; Gref, R. Novel Core(polyester)−Shell(polysaccride) Nanoparticles: Protein Loading and Surface Modification with Lectins. *J. Controlled Release* **2003**, *92*, 103–112.
19. Sihorkar, V.; Vyas, S. P. Potential of Polysaccride Anchored Liposomes in Drug Delivery, Targeting and Immunization. *J. Pharm. Pharm. Sci.* **2001**, *4*, 138–158.
20. Pelletier, S.; Hubert, P.; Lapicque, F.; Payan, E.; Dellacherie, E. Amphiphilic Derivatives of Sodium Alginate and Hyaluronate: Synthesis and Physico-Chemical Properties of Aqueous Dilute Solutions. *Carbohydr. Polym.* **2000**, *43*, 343–349.
21. Mocanu, G.; Mihai, D.; Picton, L.; Leharf., D.; Muller, G. Associative Pullulan Gels and Their Interaction with Biological Active Substances. *J. Controlled Release* **2002**, *83*, 41–51.
22. Erlich, R. B.; Werneck, C. C.; Mourao, P. A. S. Major Glycosaminoglycan Species in the Developing Retina: Synthesis, Tissue Distribution and Effects Upon Cell Death. *Exp. Eye Res.* **2003**, *77*, 157–165.
23. Pieper, J. S.; Van, Wachem, P. B.; Van, Luyn, M. J. A.; Brouwer, L. A.; Hafamans, T.; Veerkamp, J. H.; Van, Kuppevelt, T. H. Attachment of Glycosaminoglycans to Collagenous Matrices Modulates the Tissue Response in Rats. *Biomaterials* **2000**, *21*, 689–699.
24. Kirker, K. R.; Luo, Y.; Nielson, J. H.; Shelby, J.; Prestwich, G. D. Glycosamino-glycan Hydrogel Films as Bio-interactive Dressings for Wound Healing. *Biomaterials* **2002**, *23*, 3661–3671.
25. Henke, C. A.; Roongta, U.; Mickelson, D. J.; Knutson, J. R.; McCarthy, J. B. CD44-Related Chondroitin Sulfate Proteoglycan, A Cell Surface Receptor Implicated with Tumor Cell Invasion, Mediates Endothelial Cell Migration on Fibrinogen and Invasion into a Fibrin Matrix. *J. Clin. Invest.* **1996**, *97*, 2541–2452.
26. Mishra, S.; Webster, P.; Davis, M. E. Pegylation Significantly Affects Cellular Uptake and Intracellular Trafficking of Non-viral Gene Delivery Particles. *Eur. J. Cell. Biol.* **2004**, *83*, 97–111.
27. Nimesh, S.; Goyal, A.; Pawar, V.; Jayaraman, S.; Kumar, P.; Chandra, R.; Singh, Y.; Gupta, K. C. Polyethylenimine Nanoparticles as Efficient Transfecting Agents for Mammalian Cells. *J. Controlled Release* **2006**, *110*, 457–446.

28. Gabrielson, N. P.; Pack, D. W. Acetylation of Polyethylenimine Enhances Gene Delivery *via* Weakened Polymer/DNA Interactions. *Biomacromolecules* **2006**, *7*, 2427–2435.
29. Lemarchand, C.; Gref, R.; Passirani, C.; Garcion, E.; Petri, B.; Müller, R.; Costantini, D.; Couvreur, P. Influence of Polysaccharide Coating on the Interactions of Nanoparticles with Biological Systems. *Biomaterials* **2006**, *27*, 108–118.
30. Fujimoto, T.; Kawashima, H.; Tanaka, T.; Hirose, M.; Toyama-Sorimachi, N.; Matsuzawa, Y.; Miyasaka, M. CD44 Binds a Chondroitin Sulfate Proteoglycan, Aggrecan. *Int. Immunol.* **2001**, *3*, 359–366.
31. Simões, S.; Slepushkin, V.; Pires, P.; Gaspar, R.; Pedroso de Lima, M. C.; Düzgüne, N. Human Serum Albumin Enhances DNA Transfection by Lipoplexes and Confers Resistance to Inhibition by Serum. *Biochim. Biophys. Acta* **2000**, *1463*, 459–469.
32. Moore, N. M.; Barbour, T. R.; Sakiyama-Elbert, S. E. Synthesis and Characterization of Four-Arm Poly(ethylene glycol)-Based Gene Delivery Vehicles Coupled to Integrin and DNA-Binding Peptides. *Mol. Pharmaceutics* **2008**, *5*, 140–150.
33. Ogris, M.; Brunner, S.; Schuller, S.; Kircheis, R.; Wagner, E. Pegylated DNA/Transferrin-PEI Complexes: Reduced Interaction with Blood Components, Extended Circulation in Blood and Potential for Systemic Gene Delivery. *Gene Ther.* **1999**, *6*, 595–605.
34. Swami, A.; Kurupati, R. K.; Pathak, A.; Singh, Y.; Kumar, P.; Gupta, K. C. A Unique and Highly Efficient Non-viral DNA/siRNA Delivery System Based on PEI-Bisepoxide Nanoparticles. *Biochem. Biophys. Res. Commun.* **2007**, *362*, 835–841.
35. Godbey, W. T.; Kenneth, K. W.; Mikos, A. G. Tracking the Intracellular Path of Poly(ethylenimine)/DNA Complexes for Gene Delivery. *Proc. Natl. Acad. Sci. U.S.A.* **1999**, *96*, 5177–5181.
36. Reddy, L. H.; Sharma, R. K.; Murthy, R. S. R. Enhanced Tumour Uptake of Doxorubicin B Loaded Poly(butyl cynoacrylate) Nanoparticles in Mice Bearing Dalton's Lymphoma Tumors. *J. Drug Target.* **2004**, *2*, 443–451.
37. Thakkar, H.; Sharma, R. K.; Mishra, A. K.; Chuttani, K.; Murthy, R. S. R. Efficiency of Chitosan Microspheres for Controlled Intra-articular Delivery of Celecoxib in Inflammed Joints. *J. Pharm. Pharmcol.* **2004**, *56*, 1091–1099.
38. Reddy, L. H.; Sharma, R. K.; Chuttani, K.; Mishra, A. K.; Murthy, R. S. R. Influence of Administration Route on Tumour Uptake and Biodistribution of Etoposide Loaded Solid Lipid Nanoparticles in Dalton's Lymphoma Tumor Bearing Mice. *J. Controlled Release* **2005**, *105*, 185–198.
39. Eck, S. L.; Wilson, J. M. In *The Pharmacological Basis of Therapeutics*; Gilman, A. G., Goodmann, L. S., Eds.; Macmillan Publishing Co.: New York, 2005; pp 77−102.
40. Zeng, C.; Toole, B. P.; Kinney, S. D.; Kuo, J.; Stamenkovic, I. Inhibition of Tumor Growth *In Vivo* by Hyaluronan Oligomer. *Int. J. Cancer.* **1998**, *77*, 369–401.
41. Lesley, J.; Hascall, V. C.; Tammi, M.; Hyman, R. Hyaluronan Binding by Cell Surface CD44. *J. Biol. Chem.* **2000**, *275*, 267–269.
42. Anghileri, L. J. *In Vivo* Synthesis of Acid Mucopolysaccharides by Ehrlich Ascites Tumor Cells. *J. Cancer Res. Clin. Oncol.* **1976**, *88*, 17–24.
43. Underhill, C. CD44: The Hyaluronan Receptor. *J. Cell. Sci.* **1992**, *103*, 293–298.
44. Peach, R. J.; Hollenbaugh, D.; Stamenkovic, I.; Aruffo, A. Identification of Hyaluronic Acid Binding Sites in the Extracellular Domain of CD44. *J. Cell Biol.* **1993**, *122*, 257–264.
45. Jalkanen, S.; Jalkanen, M.; Bargatze, R.; Tammi, M.; Butcher, E. C. Biochemical Properties of Glycoproteins Involved in Lymphocyte Recognition of High Endothelial Venules in Man. *J. Immunol.* **1988**, *141*, 1615–1623.
46. Stamenkovic, I.; Amiot, M.; Pesando, J. M.; Seed, B. A Lymphocyte Molecule Implicated in Lymph Node Homing is a Member of the Cartilage Link Protein Family. *Cell* **1989**, *56*, 1057–1062.
47. Goldstein, L. A.; Zhou, D. F. H.; Picker, L. J.; Minty, C. N.; Bargatze, R. F.; Ding, J. F.; Butcher, E. C. A Human Lymphocyte Homing Receptor, the Hermes Antigen, is Related to Cartilage Proteoglycan Core and Link Proteins. *Cell* **1990**, *56*, 1063–1072.
48. Takei, Y.; Maruyama, A.; Ferdous, A.; Nishimura, Y.; Kawano, S.; Ikejima, K.; Okumura, S.; Asayama, S.; Nogawa, M.; Hashimoto, M.; Makino, Y.; Kinoshita, M.; Watanabe, S.; Akaike, T.; Lemasters, J. J.; Sato, N. Targeted Gene Delivery to Sinusoidal Endothelial Cells: DNA Nanoassociate Bearing Hyaluronan-Glycocalyx. *FASEB J.* **2004**, *18*, 699–701.
49. Henke, C. A.; Roongta, U.; Mickelson, D. J.; Knutson, J. R.; McCarthy, J. B. CD44-Related Chondroitin Sulfate Proteoglycan, A Cell Surface Receptor Implicated with Tumor Cell Invasion, Mediates Endothelial Cell Migration on Fibrinogen and Invasion into a Fibrin Matrix. *J. Clin. Invest.* **1996**, *97*, 2541–2552.
50. Zhang, X. Q.; Wang, X. L.; Zhang, P. C.; Liu, Z. L.; Zhuo, R. X.; Mao, H. Q.; Leong, K. W. Galactosylated Ternary DNA/Polyphospharamidate Nanoparticles Mediate High Gene Transfection Efficiency in Hepatocytes. *J. Controlled Release* **2005**, *102*, 749–763.
51. Lee, M; Nah, J. W.; Kwon, Y.; Koh, J. J.; Ko, K. S.; Kim, S. W. Water Soluble and Low Molecular Weight Chitosan Based Gene Delivery. *Pharm. Res.* **2001**, *8*, 427–431.
52. Tseng, W. C.; Tang, C. H.; Fang, T. Y. The Role of Dextran Conjugation in Transfection Mediated by Dextran-Grafted Polyethylenimine. *J. Gene Med.* **2004**, *6*, 895–905.